Pak. J. Bot., 58(2): 421-427, February 2026.

ARTICLE | DOI: http://dx.doi.org/10.30848/PJB2026-2(10)

ROOT DEGRADATION OF THE EPIPHYTIC PLANT *TILLANDSIA IONANTHA* AND ITS EXCLUSION AGAINST FOUR HEAVY METALS

YUANYUAN LIU[#], SHUO HAN[#], ZHEN TANG, GUILING ZHENG AND PENG LI*

School of Resources and Environment, Qingdao Agricultural University, Qingdao 266109, Shandong, China
#Equal first author

*Corresponding author's email: pengleep@qau.edu.cn

Abstract

Epiphytic *Tillandsia* mainly uses its leaves to absorb water and nutrients from the air, so its root structure and function is rare studied. In this study, *T. ionantha* was used as the material to study the structure changes from the primary root to mature root, and to assess whether the roots have retention capacity of the heavy metals like the leaves. Results showed that the basic structure of the mature root system is the same as that of the primary root, composing of epidermal cells, the cortex, and vascular columns. With the maturity of the root system, these root structures change significantly. The epidermis thickens, the epidermal cells are broken, the cortical tissue begins to harden, the vascular column and the cortical cells are broken, an obvious hollow appears, and the inside of the cell changes from containing many organelles to having almost no organelles. These phenomena indicate that there is a gradual degradation process from vital to non-vital during the root growth of *T. ionantha*. The root surface of the mature roots of *T. ionantha* showed a certain degree of adsorption of the four metals, whereas the metal element content in the roots was not significantly different from the control. The results indicated that the root system of *Tillandsia* had an obvious exclusion capacity for the four metals, which was closely related to the degradation of the root system and the loss of its ability to transport nutrients.

Key words: Epiphytes; Heavy metal; Root structure; Surface adsorption

Introduction

Tillandsia is native to Central and South America, has high ornamental value, and does not need soil to grow (Benzing, 2000). It has been widely introduced and cultivated all over the world. As a special epiphyte group, *Tillandsia* mainly uses its leaves to absorb water and nutrients from the air (Pierce *et al.*, 2001; Raux *et al.*, 2020), so the leaves have a strong absorption capacity. It has strong leaf absorption efficiency for many pollutants in the atmosphere, especially heavy metals (Markert *et al.*, 2001; Figueiredo *et al.*, 2004), thus becoming an "indicator plant" for the sensitive detection of atmospheric heavy metal contamination (Schreck *et al.*, 2020; Falsini *et al.*, 2022). Calasans & Malm (1997) found that *T. usneoides* can quickly and efficiently accumulate mercury ions that float in air. Sun *et al*., (2021) demonstrated that the majority of Hg particles were predominantly adsorbed by leaf trichomes with limited translocation to internal tissues, establishing trichomes as the principal sites for heavy metal adsorption in epiphytic *Tillandsia* species. Wannaz *et al*., (2006) demonstrated that *T. capillaris* and *T. tricholepis* can effectively absorb Pb, Ni, Fe, Zn, Cu, S, and other atmospheric elements. Subsequent experiments have shown that other common heavy metal elements in the atmosphere, such as Mn, Cd, Co, and the nuclides Cs, Sr, and Rn, as well as organic pollutants such as formaldehyde, polycyclic aromatic hydrocarbons, and polychlorinated biphenyls, can also be monitored using the absorption mechanisms of different *Tillandsia* leaves (Vianna *et al.*, 2011; Zheng *et al.*, 2017; Li *et al.*, 2019).

Compared to powerful leaves, the *Tillandsia* root system is thought to be fixed, and its original absorption function is degraded (Benzing, 2000). In other words, the root system of *Tillandsia* does not absorb water, nutrients and heavy metals. However, owing to the degradation of root function, little attention has been paid to the root structure of *Tillandsia*. Brighigna (1990) compared the structure of both free and anchoring roots and found the presence in the rootcap of mucopolysaccharidic material, whose hydrophilic nature is well suited for contact with the support. Benzing (2000) argued that in the evolutionary history of the *Tillandsia*, when foliar trichomes acquired the function of absorbing water and nutrients, the function of anchoring the plant to the substrate fell to the roots. Segecin & Scatena (2004) described the rhizomes of a number of *Tillandsia* and argued that they may be an adaptation to the epiphytic habit. Males (2016) proved that in some epiphytic *Tillandsia*, the roots are severely hardened, a feature that precludes any significant absorptive role, exerts a fixative effect and maintains an association with the plant.

However, the root structure and function in *Tillandsia* is only investigated in the mature root system. Whether the primary root has vitality and absorption ability, and the change of root structure during the growth process has rarely been studied. Therefore, in this study, *T. ionantha* was used as the material to study the structure changes from the primary root to mature, and to assess whether they have retention capacity of the heavy metals like the leaves.

Received: 04-09-2024 | Revised: 16-05-2025 | Accepted: 25-05-2025 | Online: 24-10-2025

Material and Methods

Experimental materials: *T. ionantha* is a perennial herb of the genus *Tillandsia* in the family Bromeliaceae and is distributed in the United States, Mexico, and southern Argentina (Till & Vitek, 1985; Pinto *et al.*, 2006). This unique plant possesses leaves that are densely covered with white scales that help absorb water and nutrients from the air (Benzing *et al.*, 1976).

Root structure analysis of the *T. ionantha*

SEM analysis: A group of roots from the primary and mature roots of *Tillandsia* was cleaned, fixed with 4% glutaraldehyde for 48 h, and then dehydrated with 30%, 50%, 70%, 80%, 90%, and 100% (2 times) gradient volume fractions of alcohol for 10 min. Immediately after dehydration, the sample was fixed to a carrier fragment and placed in an airtight container for natural drying (Rudrappa *et al.*, 2008). The surface and internal structure of the primary and mature roots were observed by SEM (JSM-7500F, JEOL Ltd., Japan), and the images were observed under the field of view of the electron microscope. The length and width of 10 epidermal cells, diameter of 10 outer cortices, endothelial and mid-column cells, and density of bacilli and cocci per unit area of five units were measured.

TEM analysis: A group of *Tillandsia* primary and mature roots were washed and placed in phosphate buffer for 2 h. These were rinsed thrice with 0.1 M phosphoric acid rinse solution for 15 min, fixed with 1% osmium acid fixative solution for 2-3 h, and rinsed three times with 0.1 M phosphoric acid rinse solution for 15 min. After that, they were dehydrated with 50%, 70%, 90% ethanol, and 90% acetone (1:1), 90% acetone, and 100% acetone gradients. Except for the last set which was performed at room temperature, all experiments were performed at 4°C, embedded and cured in an oven, sectioned with an ultramicrotome for 70 nm, and the internal organelle structure of air brometon root cells was observed under the field of transmission electron microscopy (HT7700, Hitachi, Japan).

Absorption of heavy metals by the root system of Tillandsia

Treatment method: Four heavy metals-Al, Pb, Cu, and Ni-were selected for treatment; the solutions used were $AlCl_3 \cdot 6H_2O$, lead nitrate, copper sulfate, and nickel standard solutions. Three strains of *T. ionantha* with similar growth and developmental conditions were used for each metal solution treatment, and their roots were soaked in the metal solution. The concentration of the metal solution was set at 1 mM, the pH was adjusted to 4.8 with dilute hydrochloric acid, and the treatment time was 6 h. In addition, three plants without the metal solution stress treatment were used as controls.

Determination of the heavy metal content adsorbed on root surface: After the metal stress treatment of *T. ionantha*, the root surface was cleaned with deionized water, the wash was fixed and stored, and the concentrations of the four metals in the wash were determined by the atomic absorption method (AA-7000F, Shimadzu, Japan).

Measurement conditions: Al: wavelength 324.8 nm, lamp current 3.0 mA, slit 0.5 nm, burner height 6.0 mm, acetylene flow rate 1.8 L/min, air pressure 0.25 Mpa.

Pb: wavelength 283.3 nm, drying temperature 100–120°C, lasting 20 seconds; Ashing temperature 400-750°C for 20-25 seconds; Atomization temperature 1700–2000°C for 4-5 seconds.

Cu: Measurement conditions: detection wavelength of 324.7 nm, air-acetylene flame with background correction, if necessary.

Ni: Flame atomic absorption spectrophotometry for Ni determination in soil. Using the 232.0 nm line as the absorption line, there were three Ni wires with very close wavelength distances, which should be overcome using a narrow spectral passband.

Determination of heavy metal content in the roots: Washed roots were weighed to 2.0 g, placed in a constant temperature drying oven at 45°C, and crushed. Then, 0.2 g of the sample was weighed into a digester, and 8 mL of nitric acid and 2 mL of perchloric acid were added, shaken well, sealed with a surface dish, and left overnight. The next day, it was heated and digested at a constant temperature of 70 °C in the digester. The samples were shaken well every half hour until they were clarified, digested, and allowed to cool to room temperature. Deionized water was added to a final volume of 25 mL, shaken well, and allowed to wait for testing. Three blank test solutions were prepared using the same procedure. Finally, the atomic absorption method was used to determine the content of the four metals in the sample.

Statistical methods: Photoshop 7.0 (Adobe, USA) was used to measure and annotate the cell size observed by SEM, and Excel and SPSS 26.0 (IBM, USA) were used to process the data and analyze the significance of the differences.

Results and Discussion

Primary root structure: SEM observations showed that the roots of *T. ionantha* were round and composed of epidermal cells, cortical tissues (including the outer cortex and endothelial cortex), and a vascular column (including the stele and pericycle) (Fig. 1A). Various types of root surface microorganisms were also found on the root surface. TEM microscopy revealed that the cells contained various organelles.

Epidermal cells: SEM analysis showed that the root surface was smooth and without root hairs and that the epidermal cells were monolayer cells with an obvious shape and regular distribution, mostly pentagonal or hexagonal (Fig. 1B, C); the measured epidermal cell length was 41.24 ± 7.41 μm and the width was 22.38 ± 2.77 μm ($n = 10$), which showed that the difference in epidermal cell length was large, while the difference in the width of individual cells was relatively small.

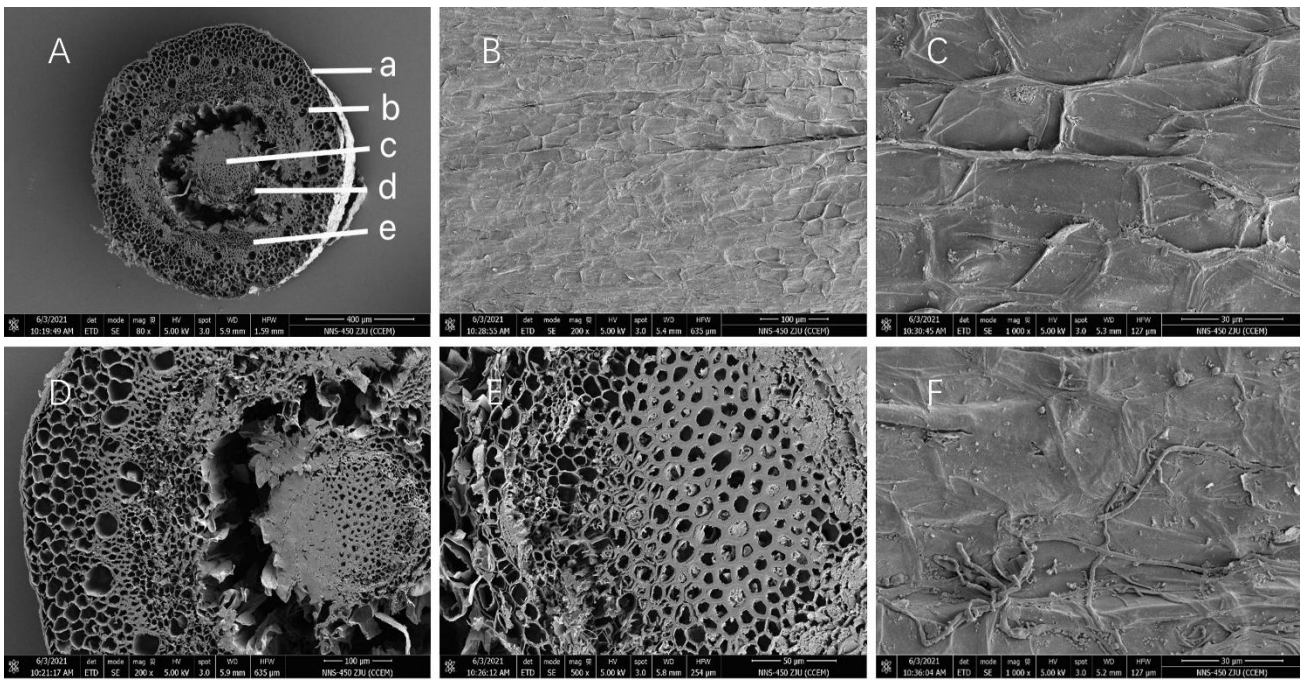

Fig. 1. SEM observation of primary roots in *T. ionantha.*
A, *T. ionantha* root cross-section; **B,** *T. ionantha* primary root epidermal cells; **C,** Enlarged epidermal cells; **D,** Cortical tissue cross-sectional detail; **E,** Vascular column section detail; **F,** Rhizosphere microorganisms attached to the root surface
Note: a, epidermis; b, integular; c, center column; d, middle column sheath; e, endothelial layer.

Cortical tissue: The cortical tissue consisted of an outer cortex and an endodermis, both of which were formed by round thin-walled cells of varying sizes and regular shapes, with a clear distinction between the inner and outer cortex; the outer cortex consisted of 5-6 layers of larger thin-walled cells that were not tightly packed, and the endodermis cells were smaller and tightly packed (Fig. 1D). Compared to the endodermal cells the outer cortex cells were much more regular in shape, with an outer cortex cell diameter of 25.37 ± 4.60 μm (n = 10) and an inner cortex cell diameter of 13.04 ± 2.45 μm (n = 10). That is, the endodermal cells were roughly half the size of the exodermal cells. The endodermis was lignified and the cell walls were significantly thickened with large thin-walled cells in the middle.The endothelial layer was lignified, and the cell wall was markedly thickened, with large parenchymal cells in between. The cells were tightly arranged with no intercellular space and rings with thick-walled histiocytes were observed (Fig. 1D), blocking the cortex and dividing it into two regions with thickened secondary walls and reduced lumens (Proença *et al.*, 2008).

Vascular column: There is a clear boundary between the vascular area and the cortex, the vascular column contains the stele, which is defined by the pericycle formed by parenchyma cells, and the stele cells are composed of thick-walled cells with small and compact arrangement (Fig. 1E), and 10 stele cells were randomly selected and measured to be 8.03 ± 1.26 μm in diameter, which is different from the diameter of the parenchyma cells in the cortex, but the size is more uniform. The lack of ductal differentiation in the stele and limited transport function also reflects the characteristics of *Tillandsia* root degradation.

In the *Tillandsia* root system, the mid-column is limited by lignified cell loops, which in the current study are interpreted as a mid-column sheath. The pericycle is partially hollow because of dry cracking, and the connection with the cortical cells is not tight. The pericycle is relatively scattered, and the part of the pericycle cells closer to the endothelial layer is larger, and many even cause rupture, which is also a characteristic of the *Tillandsia* root system in the degradation process.

Root surface microorganisms: Colonies appeared on the surface of the root system of the empty phoenix; the spores were assessed by observing the morphology and size of the colonies, measuring the colony density, and observing the characteristics of spores, spore peduncle morphology, and size. It was evident that the spores were produced, and the spore peduncles were vertically symmetrical and numerous, and the spores were solitary or clustered, spherical, or ovate (Fig. 1F). The densities of bacilli and cocci were 0.012 ± 0.006 cells/μm^2 and 0.031 ± 0.016 cells/μm^2, respectively. Cocci are small, dense, and tend to cluster near bacilli; some bacilli are longer, some even reaching up to 57.22 μm in length.

Internal structure of the cell: In the internal structure of the cells, a large number of organelles were observed using TEM (Fig. 2A). There were clusters of vesicles with many vacuoles and some without boundaries. Some vacuoles were fused together. Clusters or isolated electron-transparent vesicles were visible, which were not bound by any membrane but were surrounded by a partially black substance; some of these vesicles appeared to merge with the vacuoles (Fig. 2C, D). They became larger as they moved closer to the vacuolar body. The endoplasmic reticulum (ER) is abundant with rough surface elements often parallel to the cell wall (Fig. 2B).

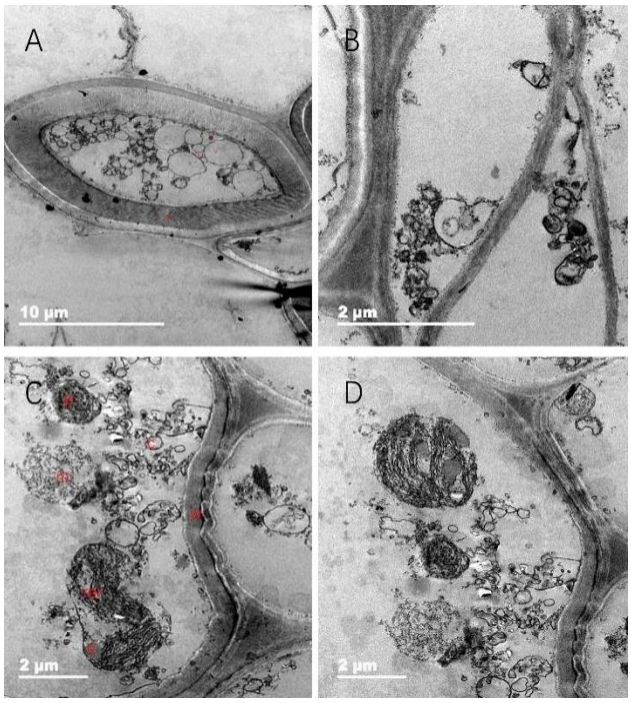

Fig. 2. Intracellular structure of TEM in primary root system of *T. ionantha.*
A, Intact cell structure; **B,** Small vesicles; **C,** More pronounced organelles; **D,** Amplified organelles.
Note: p- cytoplasm; n- nucleolus; v- vacuole; c-vesicle; w-cell wall; m-mitochondria; rer-rough endoplasmic reticulum

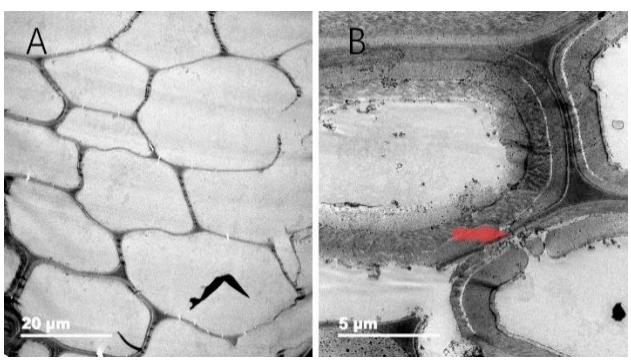

Fig. 4. Internal cell structure of TEM of mature roots in *T. ionantha.*
A, Partial degraded cells; **B,** Schematic diagram of intercellular filaments

The free mitochondria and nucleoli of the nucleus were distinct, but the whole nucleus was not clear in this TEM. Part of the cell wall was thin (Fig. 2B); in the thick segment of the cell wall, the outer layer was elevated (Fig. 2A). In living cells, the endoplasmic reticulum surrounded part of the cytoplasm.

Mature root structure: SEM analysis of mature root structure showed that the nascent yellow roots and mature roots were both similar and significantly different. The root structure is composed of epidermal cells, the cortex, and vascular columns (Figs. 1 and 3). However, these three root structures change significantly with the maturity of the root system.

Epidermal cells: The surface of the root system of *T. ionantha* had many dry cracks, and the surface was no longer flat and smooth but became uneven (Fig. 3A). The epidermis of mature roots becomes thicker, the epidermal cells have different degrees of degradation, their contours are no longer obvious, there are many broken cells, and the cell area also becomes larger (because the epidermal cell boundaries are no longer evident and cannot be measured concretely) (Fig. 3B).

Cortical tissue: Overall, the cortical tissue thinned, leaving the cell wall to thicken as the epidermis ages (Fig. 3C). The inner layer had parenchyma cells, the outer cortex exhibited sclerosis, and the cells of the endothelial layer had thickened vertical and peripheral walls. The shape of the cells in the outer cortex changed from the regular round shape of the primary root system to an irregular square.

The diameters of 10 outer cortex and endothelial cells were measured and compared with the sizes of the inner and outer epidermal cells of the primary root system. Analysis of the changes in degenerated cortical histiocytes. The cell size of the inner and outer cortices of mature roots did not change considerably from those of the primary roots, but the cell size did change (Table 1).

The endothelial layer was lignified, the cell wall was significantly thickened, the intercellular space became smaller, the cells were smaller, and some cells degenerated into thick cell walls.

Vascular column: The vascular column is composed of a stele and a pericycle; however, the stele gradually becomes smaller and disappears during the development of mature roots, and the stele cells become significantly larger than those of the primary roots, changing from thick-walled cells to parenchyma cells. There were fewer and more fragmented cells in the pericycle (Fig. 3E). The column sheath and endothelial cells in the primary root system were also partially hollow, which may be a characteristic of the gradual degradation of the *T. ionantha* root system.

Root surface microorganisms: In general, the number of root surface microorganisms in mature roots increased, and the number of microbial species increased significantly compared with that in the primary roots. Various microorganisms with few or no microorganisms in the primary root system were added, and the number of flattened strains increased significantly. Without a large number of accumulated bacilli, the spores were no longer distinct; there were still a large number of cocci distributed in the clusters, and a large number of cocci were present around the bacilli (Fig. 3F).

Compared with that in the primary roots, the density of surface bacilli and cocci in mature roots decreased and were unevenly distributed, and there were no larger bacilli. (Table 2) It can be observed that cocci are clustered around other fungi, similar to the primary root system.

The types and densities of microorganisms on the surface of mature roots and primary roots are different, and these microorganisms may promote plant growth, prevent the erosion and poisoning of plant roots by other molds, and improve plant resistance to stress (Wei *et al.*, 2015; Pimentel *et al.*, 2020).

Table 1. Diameters of different root cells in *T. ionantha.*

Cell type	Diameter (μm) (n = 10)
Primary root epidermal cell length	41.24 ± 7.41
Primary root epidermal cell width	22.38 ± 2.77
Primary root outer cortical cells	25.37 ± 4.60
Primary root endothelial cells	13.04 ± 2.45
Mature root outer epidermal cells	27.29 ± 7.15
Mature root inner epidermal cells	10.10 ± 7.93
Primary root mid-column cells	8.03 ± 1.26

Table 2. Comparison of microbial density on root surface in *T. ionantha.*

Category of bacteria	Density (cells/μm^2)
Primary root surface cocci	0.031 ± 0.016
Primary root surface bacillus	0.012 ± 0.006
Mature root surface cocci	0.019 ± 0.009
Mature root surface bacillus	0.009 ± 0.004

Internal structure of the cell: Within the internal structure of the root cell, a large cell cavity can be seen in the vestigial cells, and some cells show extensive cytoplasmic vacuolization, with only few organelles and a large number of amorphous vesicular substances in the cavity. Part of the plasmodesmata runs through two adjacent cell walls, between which the cytoplasm flows, making it a symplast (Fig. 4B). It is important to note that dead cells are present in *Tillandsia* and are left to form a covering consisting of highly compressed cell walls. Many studies have shown that the cell wall prevents harmful substances, such as heavy metals, from entering the cell, thereby improving plant tolerance to heavy metals (Huckelhoven, 2007; Roberts, 2001; Chen *et al.*, 2003). These dead cells may reduce the ability of *Tillandsia* root systems to absorb nutrients and heavy metals.

In summary, compared with that of the primary roots, the epidermis of the mature roots of *T. ionantha* was thick, the epidermal cells were broken, the cortical tissue began to harden, the vascular column and the cortical cells were broken, an obvious hollowing phenomenon appeared, and the inside of the cell changed from containing many organelles to having almost no organelles. These phenomena indicate that the root system of *T. ionantha* underwent obvious degeneration, from a viable organ to a non-viable degenerative organ, with only an attachment effect. Meanwhile, it also shows that the root cells of *Tillandsia* are not inactive at the beginning but have an obvious degeneration process.

Absorption of heavy metals by mature roots of *Tillandsia*: Analysis of adsorption metal content on the root surface of the *T. ionantha*: The data of atomic absorption experiment showed that the contents of Al, Cu, Ni, and Pb on the root surface of the aqueous solution-treated *T. ionantha* were 2.83, 3.47, 0.55 and 12.14 μg/g, respectively, indicating that the metal elements in the air are adsorbed to varying degrees by the roots of *T. ionantha*. After treating the roots of *T. ionantha* with a single metal solution, the corresponding metal element content on the root surface increased significantly (p<0.05), and the contents of other metal elements did not change significantly compared with the control (Table 3). This indicates that the root epidermis had a certain degree of adsorption of the corresponding metal elements. This may be related to the number and density of fungi on the root surface, and studies have shown that the mycelium on the root surface has a strong ability to absorb heavy metals and has the ability to prevent heavy metals from entering the plant (Chen *et al.*, 2003).

Analysis of metal content in the root system of the *Tillandsia*: The contents of Al, Cu, Ni, and Pb in the roots of *Tillandsia* treated with aqueous solution were 2.60, 3.34, 0.53, and 11.92 μg/g, respectively. After treatment with the four metals, there was no significant increase in the corresponding metal element content in the root system (p>0.05), and the contents of other metal elements did not change significantly compared with the control (p>0.05) (Table 4). This indicated that these four metals did not enter the root system of *T. ionantha* when the plant was treated with a single metal solution.

In other words, the surface of the *T. ionantha* root system will have different degrees of surface adsorption of metal elements but will not absorb metal elements into the root. The evidence further verifies the existence of root degradation in *Tillandsia* and the loss of the ability to transport nutrients from the side of the characteristics, coinciding with our previous observation of the *T. ionantha* root system structure changes (Figs. 2, 3).

Table 3. Concentrations of adsorbed metals on the surface of *Tillandsia* roots

Metal concentration	Al (μg/g)	Cu (μg/g)	Ni (μg/g)	Pb (μg/g)
Control	2.83 ± 0.31^b	3.47 ± 0.41^b	0.55 ± 0.28^b	12.14 ± 0.29^b
Al treatment	7.98 ± 0.67^a	3.48 ± 0.43^b	0.53 ± 0.28^b	12.26 ± 0.30^b
Cu treatment	2.83 ± 0.36^b	23.13 ± 0.70^a	0.57 ± 0.29^b	12.21 ± 0.31^b
Ni treatment	2.82 ± 0.35^b	3.47 ± 0.42^b	14.65 ± 0.54^a	12.19 ± 0.34^b
Pb treatment	2.83 ± 0.30^b	3.47 ± 0.44^b	0.55 ± 0.35^b	15.89 ± 0.42^a

Note: The different letters a and b indicate that there is a significant difference in the content of the same element between different treatments, and there is no significant difference between the same letters

Table 4. Metal concentrations in *Tillandsia* roots.

Metal concentration	Al (μg/g)	Cu (μg/g)	Ni (μg/g)	Pb (μg/g)
Contrast	2.60 ± 0.64^a	3.34 ± 0.32^a	0.53 ± 0.02^a	11.92 ± 0.32^a
Al treatment	2.63 ± 0.37^a	3.35 ± 0.35^a	0.53 ± 0.02^a	11.94 ± 0.35^a
Cu treatment	2.61 ± 0.28^a	3.43 ± 0.38^a	0.52 ± 0.04^a	11.93 ± 0.45^a
Ni treatment	2.61 ± 0.34^a	3.35 ± 0.32^a	0.54 ± 0.04^a	11.95 ± 0.46^a
Pb treatment	2.61 ± 0.39^a	3.35 ± 0.35^a	0.53 ± 0.03^a	12.10 ± 0.47^a

Note: a indicates that there is no significant difference in the content of the same heavy metal between different treatments in the same column

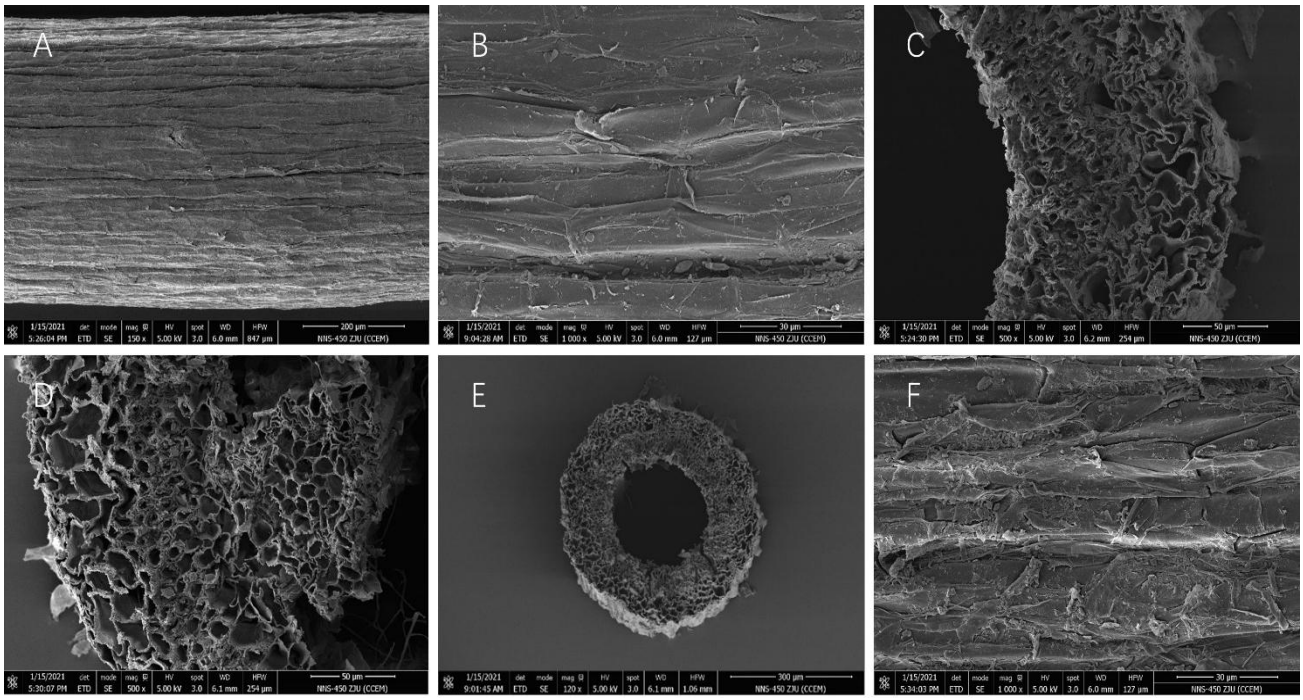

Fig. 3. SEM structure of mature roots in *T. ionantha.*
A, Mature root surface; **B,** Mature root epidermal cells; **C,** Partial detail of mature root cortex; **D,** Incompletely degraded middle column; **E,** Fully degenerated middle column; **F,** Root surface microorganisms of degenerated roots.

Conclusion

SEM, TEM analysis show that, with the maturation of the root system, the root structure of *T. ionantha* has a series of distinct changes, including that the root epidermis becomes thicker, the epidermal cells appear broken phenomenon, the cortical tissues begin to harden, the vascular column and the cortical cells fracture, the cell interior changes from containing a lot of organelles to almost no organelles. These phenomena indicate that the root system of the *T. ionantha* has a growth process from vitality to lifelessness, and gradually degraded, although the *T. ionantha* mature root system and the primary root system have the same basic structure. The absorption experiment of four kinds of heavy metals further verified this point. When the *T. ionantha* root system grows to maturity, only surface adsorption of heavy metals is retained, while the function of the absorption of elements into the internal root is lost. As an epiphytic plant relying on the leaves to absorb water and nutrients, the root system of *Tillandsia* mainly plays the role of fixation, which produces a special adaptation to the specific environment.

Funding: This work was supported by the National Natural Science Foundation of China (No. 32271699).

Data availability: All the data supporting the findings of this study are included in this article and in Supplementary material. Further inquiries can be directed at the corresponding author.

Author contributions: Liu YY and Han S performed the experiments and analyzed the results. Tang Z and Zheng GL analyzed the results. Li P designed the experiments. All authors wrote and edited the article.

Conflict of interest: The contact author has declared that none of the authors has any competing interests.

References

Benzing, D.H., K. Henderson, B. Kessel and J. Sulak. 1976. The absorptive capacities of bromeliad trichomes. *Amer. J. Bot.*, 63(7): 1009-1014.

Benzing, D.H. 2000. *Bromeliaceae: profile of an adaptive radiation*. Cambridge University Press.

Brighigna, L., A.C. Fiordi and M.R. Palandri. 1990. Structural comparison between free and anchored roots in *Tillandsia* (Bromeliaceae) species. *Caryologia*, 43(1): 27-42.

Calasans, C.F. and O. Malm. 1997. Elemental mercury contamination survey in a chlor-alkali plant by the use of transplanted Spanish moss, *Tillandsia usneoides* (L.). *Sci. Total Environ.*, 208(3): 165-177.

Chen, B.D., X.L. Li, H.Q. Tao, P. Christie and M.H. Wong. 2003. The role of arbuscular mycorrhiza in zinc uptake by red clover growing in a calcareous soil spiked with various quantities of zinc. *Chemosphere*, 50(6): 839-846.

Falsini, S., I. Colzi, D. Chelazzi, M. Dainelli, S. Schiff, A. Papini, A. Coppi, C. Gonnelli and S. Ristori. 2022. Plastic is in the air: Impact of micro-nanoplastics from airborne pollution on *Tillandsia usneoides* L. (*Bromeliaceae*) as a possible green sensor. *J. Hazard. Mater.*, 437: 129314.

Figueiredo, A.M.G., A.L. Alcalá, R.B. Ticianelli, M. Domingos and M. Saiki. 2004. The use of *Tillandsia usneoides* L. as bioindicator of air pollution in São Paulo, Brazil. *J. Radioanal. Nucl. Chem.*, 259: 59-63.

Hückelhoven, R. 2007. Cell wall–associated mechanisms of disease resistance and susceptibility. *Annu. Rev. Phytopathol.*, 45(1): 101-127.

Li, P., X. Sun, J. Cheng and G. Zheng. 2019. Absorption of the natural radioactive gas ^{222}Rn and its progeny ^{210}Pb by Spanish moss *Tillandsia usneoides* and its response to radiation. *Environ. Exp. Bot*., 158: 22-27.

Males, J. 2016. Think tank: water relations of Bromeliaceae in their evolutionary context. *Bot. J. Linn. Soc.*, 181(3): 415-440.

Markert, B. 2001. Determination of trace elements in *Tillandsia usneoides* by neutron activation analysis for environmental biomonitoring. *J. Radioanal. Nucl. Chem.*, 249(2): 391-395.

Pierce, S., K. Maxwell, H. Griffiths and K. Winter. 2001. Hydrophobic trichome layers and epicuticular wax powders in Bromeliaceae. *Am. J. Bot.*, 88(8): 1371-1389.

Pimentel, M.F., E. Arnão, A.J. Warner, A. Subedi, L.F. Rocha, A. Srour, J.P. Bond and A.M. Fakhoury. 2020. Trichoderma isolates inhibit Fusarium virguliforme growth, reduce root rot, and induce defense-related genes on soybean seedlings. *Plant Dis.*, 104(7): 1949-1959.

Pinto, R., I. Barría and P.A. Marquet. 2006. Geographical distribution of *Tillandsia lomas* in the Atacama Desert, northern Chile. *J. Arid Environ.*, 65(4): 543-552.

Proença, S.L. and M.D.G. Sajo. 2008. Rhizome and root anatomy of 14 species of *Bromeliaceae. Rodriguésia*, 59(1): 113-128.

Raux, P.S., S. Gravelle and J. Dumais. 2020. Design of a unidirectional water valve in *Tillandsia*. *Nat. Commun.*, 11(1): 396.

Rudrappa, T., M.L. Biedrzycki and H.P. Bais. 2008. Causes and consequences of plant-associated biofilms. *FEMS Microbiol. Ecol.*, 64(2): 153-166.

Roberts, K. 2001. How the cell wall acquired a cellular context. *Plant Physiol.*, 125(1): 127-130.

Schreck, E., J. Viers, I. Blondet, Y. Auda, M. Macouin, C. Zouiten, R. Freydier, G. Dufrechou, J. Chmeleff and J. Darrozes. 2020. *Tillandsia usneoides* as biomonitors of trace elements contents in the atmosphere of the mining district of Cartagena-La Unión (Spain): New insights for element transfer and pollution source tracing. *Chemosphere*, 241: 124955.

Segecin, S. and V.L. Scatena. 2004. Morfoanatomia de rizomas e raízes de Tillandsia L. (Bromeliaceae) dos Campos Gerais, PR, Brasil. *Rev. Bras. Bot*., 18 (2): 253-260.

Sun, X., P. Li and G. Zheng. 2021. Cellular and subcellular distribution and factors influencing the accumulation of atmospheric Hg in *Tillandsia usneoides* leaves. *J. Hazard. Mater.*, 414: 125529.

Till, W. and E. Vitek. 1985. *Tillandsia marconae*-a new species from the coastal desert of Peru. *Plant Syst. Evol.*, 149: 143-147.

Vianna, N.A., D. Gonçalves, F. Brandão, R.P. de Barros, G.M. Filho, R.O. Meire, J.P. Torres, O. Malm and L.R. Andrade. 2011. Assessment of heavy metals in the particulate matter of two Brazilian metropolitan areas by using *Tillandsia usneoides* as atmospheric biomonitor. *Environ. Sci. Pollut. Res.*, 18: 416-427.

Wannaz, E.D., H.A. Carreras, C.A. Pérez and M.L. Pignata. 2006. Assessment of heavy metal accumulation in two species of *Tillandsia* in relation to atmospheric emission sources in Argentina. *Sci. Total Environ.*, 361(1-3): 267-278.

Wei, Z., T. Yang, V. P. Friman, Y. Xu, Q. Shen and A. Jousset. 2015. Trophic network architecture of root-associated bacterial communities determines pathogen invasion and plant health. *Nat. Commun.*, 6(1): 8413.

Zheng, G., R. Pemberton and P. Li. 2017. Assessment of Cs and Sr accumulation in two epiphytic species of *Tillandsia* (Bromeliaceae) *In vitro*. *Chem. Ecol.*, 33(1): 51-60.